NASA TECHNICAL NOTE

NASA TN D-7145

DESIGN AND ANALYSIS OF
A STAR IMAGE MOTION COMPENSATOR

by K. C. Romanczyk, Aaron J. Ostroff, and W. E. Howell

Langley Research Center
Hampton, Va. 23365

NATIONAL AERONAUTICS AND SPACE ADMINISTRATION • WASHINGTON, D. C. • FEBRUARY 1973

35

1. Report No. NASA TN D-7145	2. Government Accession No.	3. Recipient's Catalog No.
4. Title and Subtitle DESIGN AND ANALYSIS OF A STAR IMAGE MOTION COMPENSATOR		5. Report Date February 1973
		6. Performing Organization Code
7. Author(s) K. C. Romanczyk, Aaron J. Ostroff, and W. E. Howell		8. Performing Organization Report No. L-8634
9. Performing Organization Name and Address NASA Langley Research Center Hampton, Va. 23365		10. Work Unit No. 188-78-57-05
		11. Contract or Grant No.
12. Sponsoring Agency Name and Address National Aeronautics and Space Administration Washington, D.C. 20546		13. Type of Report and Period Covered Technical Note
		14. Sponsoring Agency Code

15. Supplementary Notes

16. Abstract

The feasibility of designing and fabricating a small optical system to compensate for motions of a stellar field image on the focal plane of a large orbiting telescope is examined for a single-axis system. An all-reflecting two-mirror star image motion compensator maintains both a flat focal plane and image focus for one or more star images. Both theoretical and experimental evaluations show that only one adjustment is needed to aline the system since the change in focus is linearly related to the misalinements of all critical components. Results of an error analysis show that the focus error resulting from fabrication tolerances is very small compared to the adjustment capability of the system.

17. Key Words (Suggested by Author(s)) Image motion compensator Two-mirror technique Large orbiting telescopes	18. Distribution Statement Unclassified – Unlimited		
19. Security Classif. (of this report) Unclassified	20. Security Classif. (of this page) Unclassified	21. No. of Pages 32	22. Price* $3.00

DESIGN AND ANALYSIS OF A STAR IMAGE MOTION COMPENSATOR

By K. C. Romanczyk, Aaron J. Ostroff, and W. E. Howell
Langley Research Center

SUMMARY

The feasibility of designing and fabricating a small optical system to compensate for motions of a stellar field image on the focal plane of a large orbiting telescope is examined for a single-axis system. An all-reflecting two-mirror star image motion compensator maintains both a flat focal plane and image focus for one or more star images. Both theoretical and experimental evaluations show that only one adjustment is needed to aline the system since the change in focus is linearly related to the misalinements of all critical components. Results of an error analysis show that the focus error resulting from fabrication tolerances is very small compared to the adjustment capability of the system.

INTRODUCTION

The advantages of orbiting telescopes over their earth-bound counterparts have been well known by the scientific community for many years. For small orbiting telescopes, system resolution is mainly a function of the diffraction limit of the optical system. As telescope apertures increase in size, vehicle controllability plays an increasingly important function as compared to the diffraction limit of the system. For example, the resolution of a 3-meter (120-inch) diffraction-limit telescope is approximately 0.04 arc-second, whereas the probable required control stability is on the order of 0.01 arc-second (ref. 1).

Maintaining this very precise pointing accuracy is a problem of great significance. One suggested technique (ref. 2) is to use a dual-level control system, where the fine-pointing control system utilizes small optics internal to the telescope structure to stabilize all star images within the field of view to the desired accuracy. In order to accomplish this requires that the internal optics be capable of repositioning the image in two dimensions in the focal plane when the telescope is perturbed. This paper describes a system with that capability; however, the bulk of the material covers a single-axis system since the extension to two axes is straightforward.

This technique is capable of maintaining both a flat focal plane and image focus for several star images simultaneously. The design incorporates a minimum number of reflective surfaces instead of refractive components to allow dim star operations and to

1

minimize distortions. Techniques to calculate and measure the focus errors resulting from misalinement of various component parts are presented in this paper. Both theoretical and experimental results show that all errors are essentially linear and only one adjustment is needed for final alinement. An error analysis is included to determine the worst-case focus change resulting from fabrication tolerances of all components. Finally, a two-axis image motion compensation system is described.

SYMBOLS

A, B, C, . . . points on line segments

d image displacement, meters

E_m approximate error resulting from fabrication tolerance, meters

f focal length of telescope, meters

k_i coefficient of polynomial for change in optical path length (i=1, 2, 3), micrometers per degree

L_p change in optical path length, meters

M1 mirror mounted at focus of parabola (see fig. 2)

M2 mirror mounted on parabola (see fig. 2)

m dummy variable representing any misalinement error

m_i slope of line (i=1, 2, 3, 4)

p distance between mirrors M1 and M2 when 45° to optical axis, meters

r distance from single flat mirror to focal plane along optical axis, meters

t fabrication tolerance

x, y orthogonal coordinate system

α angle of mirror rotation, degrees

β angle of misalinement in mirror   M2, degrees

γ angle of misalinement in mirror   M1, degrees

δ offset distance of mirror   M2, meters

ϵ offset distance of mirror   M1, meters

ζ pointing error of telescope, radians

θ angle of misalinement in guide, degrees

λ wavelength of light, meters

ρ angle between X-axis and line connecting the focus of parabola and attachment point of mirror   M2, degrees

ϕ angle between X-axis and the direction of linear translation of mirror   M2, degrees

Bar over two letters indicates line length.

SINGLE-AXIS SOLUTION

Single-Mirror Technique

The purpose of the optical portion of an image motion compensator is to provide a method for a control system to maintain an image fixed on the focal plane despite small motions of the telescope optical axis. As shown in figure 1, the image motion compensator intersects the optical axis of the telescope to reflect incoming rays from the primary-secondary combination to the folded focal plane. In the figure, an on-axis star image is focused at point A after reflecting from a single-flat-mirror image motion compensator. If the optical axis of the telescope moves by an angle ζ, the star image moves to point B in the focal plane. The image displacement d is

$$d = f\zeta \tag{1}$$

where f is the focal length of the telescope and ζ is the rotational angle in radians. If the distance along the optical axis from the flat mirror to the focal plane is r, then the flat mirror must be rotated through an angle α given by

$$\alpha = \frac{1}{2} \tan^{-1} \frac{f\zeta}{r} \tag{2}$$

in order to compensate for ζ. Since the focal plane, as folded by the flat mirror, is a function of the flat mirror angle, it must rotate through angle 2α as the mirror rotates through α. The effect is twofold: first, the new focal plane is tilted relative to the original position and, second, the image is slightly behind the initial focal plane. Since the environment will produce focus errors from many sources, design errors should be eliminated if at all possible. Therefore, an alternate technique that minimizes the focus error has been evaluated.

Two-Mirror Technique

A two-mirror image motion compensator that eliminates the tilted focal plane problems has been designed and evaluated. The two-mirror device will intersect the optical axis of the telescope, replacing the single mirror shown in figure 1. A schematic representation of the two-mirror image motion compensator is shown in figure 2. In the illustration in figure 2(a), rays from a star are imaged on the focal plane after reflecting from two plane parallel mirrors. During actual operation the telescope will move causing all star images in the telescope field of view to be moved on the focal plane. The two mirrors will then be rotated in order to bring the star images back to the original position. For ease of experimental evaluation and discussion, the telescope has been assumed stationary and the image motion on the focal plane analyzed as a function of mirror rotation only. The two mirrors must be maintained parallel to each other as they are rotated in order to prevent the focal plane from tilting. By doing this, all stars within the field of view will be imaged on a plane that is parallel to the original focal plane, but the star images will be changed in focus. The change in focus can be eliminated if the path length from mirror M1 to the focal plane is maintained constant. This constant path length can be accomplished by translating mirror M2 as it is rotated. An illustration of this is shown in figure 2(b). Both mirrors have been rotated through the same angle and the image has been translated along the focal plane. The distance between mirrors M1 and M2 has been changed so that the total path length remains constant. It can be shown that mirror M2 is always tangent to a parabola while mirror M1 rotates on the focus of the parabola (point A, fig. 2). The concept is illustrated in figure 2(b) where the mirrors have been rotated and the image moved from point I to point H on the focal plane.

The image displacement is a function of mirror rotation angle and can be calculated by the following equation:

$$\overline{IH} = 2p \frac{\tan \alpha}{1 + \tan \alpha} \tag{3}$$

4

where $\overline{\text{IH}}$ represents the image displacement, p is the distance between the two mirrors $\overline{(\text{AB})}$ when they are both at an angle of 45° to the optic axis, and α is the mirror rotation angle from the initial 45° position. The derivation is given in the appendix.

Figure 3 contains a plot of image displacement as a function of mirror rotation angle for p = 5.08 centimeters. The mirror rotation angle α is defined to be positive when the mirror rotates in a clockwise direction. For any practical case the curve is linear for the small angles involved ($\pm 2^O$). A mirror angle of $\pm 2^O$ has been selected since this is approximately the rotation angle necessary to correct for an assumed worst-case disturbance of ± 2 arc-seconds in a 3-meter-diameter telescope operating at f/100. A 2-arc-second disturbance will cause the image to move 3.05 millimeters (ref. 3), whereas a mirror rotation angle of 2^O will allow the image to move 3.56 millimeters (eq. (3)).

A sketch illustrating the key components of the two-mirror star image motion compensator is shown in figure 4. Mirror M1 is mounted firmly to the plate and mirror M2 is mounted on two linear translation bearings which are also mounted firmly to the plate to maintain parallelism between the two mirrors but allow the distance between them to vary. The direction of linear travel of mirror M2 is always in line with the focus of a parabola. The plate rotates about a shaft which serves as the focus of the parabola, and the center of the shaft is located directly below the front surface of mirror M1. A connecting rod extends downward from mirror M2 to a guide which regulates the distance between the two mirrors as they rotate. The two mirrors, when they are not rotated, and the guide are physically located at an angle of 45° to the optical axis.

The following section includes a description of the fabrication errors associated with the two-mirror image motion compensator. The effect of these errors on system performance and the measurement technique are included.

Misalinement Analysis and Measurements

In practice any physical system has fabrication tolerances. The purpose of this section is to describe each of the possible misalinement errors and show its effect on system performance. For the image motion compensator, these misalinement errors will cause changes in the optical path length (fig. 2) with a corresponding shift of the optical focal plane. Figure 5 contains a schematic representation of the seven possible misalinement errors; each error is positive for the direction shown. The misalinement errors included

(a) Mirror M1 offset by angle γ from the ideal of 45° to the optical axis (fig. 5(a)).

(b) Front surface of mirror M1 offset by distance ϵ from the focus of the parabola (fig. 5(b)).

(c) Mirror M2 offset by angle β from the ideal of 45° to the optical axis (fig. 5(c)).

(d) Guide offset by angle θ from the ideal of 45° to the optical axis (fig. 5(d)). The guide is a physical component that is shown in figure 4.

(e) Front surface of mirror M2 offset by distance δ from the point of attachment to the guide when both mirror and guide are at 45° to the optical axis (fig. 5(e)).

(f) The imaginary line through the focus of the parabola and the attachment point of mirror M2 to the guide offset by angle ρ from the Y-axis (fig. 5(f)).

(g) Linear translation of mirror M2 offset by angle ϕ to a line through the focus of the parabola and the attachment point of mirror M2 (fig. 5(g)).

The change in path length for each error has been calculated theoretically and confirmed experimentally. In this experiment each of the errors discussed was reduced as closely to zero as possible with the use of theodolites and various reference mirrors. A Twyman-Green interferometer was then incorporated as the instrumentation to evaluate the laboratory model by measuring the change in path length (focus) as the mirrors were rotated. The interferometer system (fig. 6) basically consisted of a laser, beam splitter, and two flat mirrors. The image motion compensator is included in one leg of the interferometer and is shown enclosed in the dashed lines. Any change in focus as the mirrors are rotated causes the fringe pattern on the screen to change. Each fringe is equivalent to 0.3164 micrometer (12.5 microinches) for a wavelength λ of 0.6328 micrometer.

The physical hardware is shown in figure 7. The image motion compensator used for the experimental tests is mounted on an indexing head. The laser, beam splitter, and flat mirrors are also shown. Figure 8 contains a closeup view of the experimental model. Micrometers and screw adjustments mounted on the rear of each mirror allowed the mirror position to be varied and a motor drive system was used to automatically rotate the two mirrors.

Figure 9 is a plot of the change in path length as a function of mirror rotation angle α for several misalinement angles γ of mirror M1. (See fig. 5(a).) A positive rotation angle represents a clockwise rotation of the mirrors. The values of γ shown on the curves are very conservative since the latest version of the laboratory model has been fabricated with errors in γ that are two orders of magnitude smaller than these. The change in path length is directly proportional to the misalinement angle γ within 0.1 percent for the values tested. Although the curves are essentially linear for the small rotation angles α involved, the slope increases slightly for positive α and decreases for negative α because of the trigonometric relationships involved. All error curves exhibit the same phenomenon.

6

Each of the misalinement errors illustrated in figure 5, except the misalinement angle ϕ, has error curves similar to that shown in figure 9. The calculated and experimental data are very close for all cases. Since the derivation for each misalinement error is very cumbersome to present in a report, the calculated data have been fit to a third-order polynomial as

$$L_p = k_1\alpha + k_2\alpha^2 + k_3\alpha^3 \tag{4}$$

where L_p represents the change in optical path length in micrometers, α is the mirror rotation angle in degrees, and k_i (i=1,2,3) are the coefficients. The three coefficients are presented in table I for several values of each misalinement error; ϵ and δ are in millimeters and the other misalinement errors are in degrees. For the coefficients shown, L_p is accurate to within 0.05 micrometer.

Several conclusions can be made by analyzing the error curves (figs. 9, 10, and 11) and the coefficients in table I. The change in path length L_p is reasonably linear with respect to the mirror rotation angle α (where k_2 and k_3 are small). For a misalinement error γ of 2°, the curve is linear within 3.66 percent over a range of α from -2° to 2°. The worst-case nonlinearity for all the individual misalinement errors is 3.93 percent for $\theta = -2^{o}$ (curve not shown). The change in path length is also proportional to the misalinement error, both in magnitude and direction. For γ, ϵ, and δ, the curve is linear within 0.06 percent and L_p is symmetrical for positive and negative misalinement errors; for the other three cases (β, θ, and ρ), L_p is proportional to the misalinement error within 5 percent. The coefficients for θ and ρ are identical for opposite directions of the misalinement errors.

When a system has all linear errors, superposition holds and therefore only one adjustment is needed for alinement. One method of checking this fact and the linearity of L_p is to misaline several parameters and observe the effect. One test was to misaline γ and β by the same amount in the same direction. Analysis of the coefficients (table I) of γ and β indicates that the combined error should have coefficients that are approximately equal in magnitude to those of β alone but of opposite sign. The coefficients of the combined error are slightly different from those obtained by summing the individual errors. This difference is probably the result of the nonlinear terms. Figure 10 contains a plot of the calculated and measured change in path length as a function of α for the combined misalinement angles of γ and β.

An alined system was mounted on an indexing head and rotated 1° in a counterclockwise direction, which is approximately equivalent to misalining γ, β, θ, and ρ by -1°. The coefficients are shown in table I and a plot of L_p as a function of α is shown in

figure 11. The linearity is shown to be within 3.7 percent over the range of α from -2^O to 2^O.

The coefficients in table I and the image displacement data in figure 3 have been calculated for p = 5.08 centimeters. Equation (3) indicates that the image displacement is proportional to p. It also turns out that L_p is approximately proportional to p. Therefore, the distance p has the effect of a gain constant between image displacement and the mirror rotation angle. For example, if p is doubled, the required mirror rotation angle will be halved for the same image displacement, and the change in path length will essentially remain constant.

The image motion compensator has one nonlinear error that is a function of the direction of motion of mirror M2 (fig. 5). The linear translation of mirror M2 should be parallel with a line through the focus of the parabola and the attachment point of mirror M2 ($\phi = 0^O$). Figure 12 contains the calculated results showing the change in path length as a function of mirror rotation angle for various misalinements of angle ϕ. The calculated data show that the path length always increases or decreases parabolically, depending upon the direction of the offset angle. For an offset angle ϕ of 0.5^O and a mirror rotation angle of 2^O, the change in path length is approximately 1.1 micrometers. The next paragraphs describe a technique to determine the worst-case change in focus resulting from the combined misalinement of all components.

The data in table I have been used for an error analysis study to determine the worst-case change in path length when all the components of the image motion compensator are fixed to nominal values within a small fabrication tolerance error. The approximate error E_m resulting from each misalined component can be calculated by using the first-order term in equation (4) and by scaling the misalinement error as shown in the following equation

$$E_m = \frac{k_1 \alpha t}{m} \qquad (5)$$

where t represents the assumed fabrication tolerance and m is a dummy variable representing any of the misalinement errors.

Table II includes the values used for the error analysis and is based upon an average value for k_1 and $\alpha = 2^O$. Fabrication tolerances assumed for the analysis include angle tolerances of 30 arc-seconds and linear displacements of 7.6 micrometers (0.0003 inch). The approximate change in optical path length resulting from fabrication tolerances (excluding ϕ) is calculated to be 1.47 micrometers. This calculated value is very small and can be compensated for by rotating the entire image motion compensator (fig. 11). The rotation angle required to compensate for a change in path length of 1.47 micrometers is calculated as 1.42 arc-minutes for $\alpha = 2^O$. The change in path length for the misaline-

8

ment error ϕ is parabolic and contributes an error of only 0.02 micrometer for the specified fabrication tolerance.

The small root-sum-square error calculated in the error analysis indicates that the two-mirror star image motion compensator can be fabricated with only one adjustment to compensate for system misalinements and fabrication tolerances; the one adjustment will rotate the entire assembly. A photograph of the new fabricated model is shown in figure 13. Figure 14 is a plot of the experimentally determined error in path length as a function of mirror rotation angle for best alinement of this new model. The mirror rotation angle has been plotted over a range from -2$^\mathrm{o}$ to 2$^\mathrm{o}$. A small fluctuation and hysteresis is associated with the model; however, the root-mean-square deflection is only 1.075 micrometers. The principle of operation has been described for a light ray striking the mirror at the focus of the parabola after passing through the vertex (fig. 2) of the parabola. The only aberration that a plane mirror can introduce is focus, and it has been demonstrated in the laboratory that this system minimizes focus error for all rays parallel to the ray going through the focus of the parabola. The results are very similar to those shown in figure 14.

TWO-AXIS IMAGE MOTION COMPENSATOR

The previous discussion has been for a single-axis image motion compensator, whereas a two-axis system is required for two-axis compensation. The third axis — rotation about the optical axis — must be countered by the telescope control system.

A diagram illustrating the two-axis system is shown in figure 15. Motions of the second mirror in the first plane remain parabolic, whereas those in the other are circular; thus, the front surface of the second mirror would move tangent to the surface of a paraboloid of revolution. With this arrangement a set of images can be positioned at any desired point within the range of the compensator; however, there is a slight cross coupling between axes. For instance, if it is desired to move an image in the x-direction on the focal plane it would be necessary to rotate the two mirrors about the optical axis and also to move them along the parabola. At first glance it may appear that these motions will result in a rotation of the image; however, this is not so.

CONCLUDING REMARKS

The feasibility of design and fabrication of a small optical system to compensate for motions of several star images on the focal plane of the telescope has been demonstrated. An all-reflecting two-mirror star image motion compensator that eliminates the focal plane tilt has been fabricated, analyzed, and tested. The two mirrors are maintained parallel to each other; one mirror rotates about a central axis while the other mir-

ror rotates along a parabola. All star images within the field of view can be translated along the focal plane with essentially no change in focus since the optical path length remains constant. A Twyman-Green interferometer has been used to measure the change in path length as the mirrors rotate; for best alinement, the measured peak error was only 2.83 micrometers for a mirror motion of 2°.

Seven system misalinement errors have been analyzed theoretically and measured experimentally. From these results, it is possible to find the magnitude and direction of the focus error as a function of mirror rotation angle and misalinement. Superposition holds for this system since the combined change in focus, resulting from all misaline-ments, is linearly related to the mirror rotation angle. For this reason, only one adjust-ment is needed for final alinement. The result of an error analysis, which is based upon typical fabrication tolerances, shows that the accumulated fabrication errors will cause the optical path length to change by approximately 1.47 micrometers when the mirrors are rotated 2°.

A technique for two-axis compensation has been presented; this technique uses a minimum of two mirrors. The main change is that one of the mirrors is tangent to a surface that is a paraboloid of revolution. However, the mirror rotation required in the plane of the circle is twice as great as that required in the plane of the parabola. Also the optical path length will not vary by changing the mirror location with respect to the center of the circular plane; however, there is a slight cross coupling between the X-axis and Y-axis.

Langley Research Center,
National Aeronautics and Space Administration,
Hampton, Va., January 3, 1973.

APPENDIX

DERIVATION OF IMAGE DISPLACEMENT ALONG THE FOCAL PLANE

The image motion compensator, shown schematically in figure 16, consists of two plane parallel mirrors that are rotated in such a way as to move one or more star images along the optical focal plane. In actual practice, the telescope will move causing the star images to move along the focal plane. The two mirrors will then be rotated in order to bring the star images back to the original position. For ease of analysis, the telescope is maintained stationary and star image motion is analyzed as a function of mirror rotation. The two mirrors are maintained parallel to keep the focal plane from tilting. Also, one mirror rotates on the focus of a parabola while the second mirror is always tangent to a parabola.

A simple relationship exists between the star image displacement $\overline{IH}$ and the mirror rotation angle α for a perfectly alined star image motion compensator. For a single-axis device, star image motion along the focal plane is parallel to the X-axis. The two plane parallel mirrors are initially alined at an angle of 45° to the optic axis and have a slope

$$m_3 = \tan 135^{\circ} = -1 \tag{A1}$$

where m_3 is the slope of the original mirror position in the x,y coordinate system. By definition, the image displacement along the focal plane for a mirror rotation α is

$$\overline{IH} = I(x) - H(x) \tag{A2}$$

where $I(x)$ and $H(x)$ are the x-coordinates of points I and H. In the physical system a guide with a linear motion bearing is parallel to the original mirror plane. The point of mirror attachment to the guide is at B. As the mirror rotates, this point always moves along the guide and is the point of intersection between the original mirror position and the rotated mirror position. For this illustration, B moves to point E. The angle between the X-axis and the construction line drawn between A and E is α, and the slope m_1 of the construction line is

$$m_1 = \tan \alpha \tag{A3}$$

The light ray, which originally travels along the X-axis between A and B, changes by twice the mirror rotation angle. The deviated light ray connects points A and C and has a slope m_2 as

$$m_2 = \tan 2\alpha \tag{A4}$$

Point C is located on the rotated mirror which has a slope m_4 as

$$m_4 = \tan(135 + \alpha) \tag{A5}$$

Since the two mirrors are maintained parallel to each other, the image displacement in equation (A2) is also

$$\overline{IH} = p - C(x) \tag{A6}$$

where

$$p = A(x) - B(x) \tag{A7}$$

and since A is located at the intersection of the X-axis and Y-axis,

$$p = B(x) \tag{A8}$$

Hence, p is defined as the distance between the two mirrors when they are alined at an angle of 45° to the optic axis.

Before C(x) can be found, the x and y coordinates of E must be determined. From the intersection of lines $\overline{AE}$ and $\overline{BE}$, the coordinates of E become

$$E(x) = \frac{p}{m_1 - m_3} \tag{A9}$$

$$E(y) = \frac{pm_1}{m_1 - m_3} \tag{A10}$$

and from the intersection of lines $\overline{AC}$ and $\overline{EC}$, the x-coordinate of C is

$$C(x) = \frac{E(y) - m_4 E(x)}{m_2 - m_4} \tag{A11}$$

Substitution of equations (A9), (A10), (A11), and (A1) into equation (A6) yields

$$\overline{IH} = \frac{p\left(m_2 - m_4 - \dfrac{m_1 - m_4}{m_1 + 1}\right)}{m_2 - m_4} \tag{A12}$$

and by using the relationships

$$m_2 = \frac{2m_1}{(1 - m_1)(1 + m_1)} \qquad (A13)$$

and

$$m_4 = -\frac{1 - m_1}{1 + m_1} \qquad (A14)$$

the star image displacement becomes

$$\overline{IH} = p\,\frac{2m_1}{1 + m_1} \qquad (A15)$$

where

$$m_1 \neq -45^{\circ} \text{ or } 135^{\circ}$$

Substitution of equation (A3) into equation (A15) yields

$$\overline{IH} = 2p\,\frac{\tan \alpha}{1 + \tan \alpha} \qquad (A16)$$

which relates the mirror rotation angle to star image displacement along the optical focal plane.

REFERENCES

1. Anon.: A System Study of a Manned Orbital Telescope. D2-84042-1 (Contract NAS1-3968), Boeing Co., Oct. 1965. (Available as NASA CR-66047.)

2. Ostroff, Aaron Joel: Design of a Star Image Regulating System Utilizing a Digital Sensor. M.S. Thesis, George Washington Univ., Feb. 1971.

3. Anon.: Feasibility Study of a 120-Inch Orbiting Astronomical Telescope. AE-1148 (Contract NAS1-1305-18), J. W. Fecker Div., Amer. Optical Co. [1963]. (Available as NASA CR-66001.)

14

TABLE I

THIRD-ORDER POLYNOMIAL COEFFICIENTS

Misalinement		Coefficient		
Parameter	Error	k_1	k_2	k_3
γ	1°	-61.92	-1.08	-0.03
	2°	-123.76	-2.16	-.05
	-1°	61.92	1.08	.03
	-2°	123.76	2.16	.05
β	1°	31.50	0.55	0.01
	2°	64.04	1.12	.03
	-1°	-30.42	-.53	-.01
	-2°	-59.72	-1.04	-.02
θ	1°	-30.43	-0.51	-0.01
	2°	-59.87	-.98	-.02
	-1°	31.51	.57	.02
	-2°	64.21	1.21	.03
ρ	1°	31.51	0.57	0.02
	2°	64.21	1.21	.03
	-1°	-30.43	-.51	-.01
	-2°	-59.87	-.98	-.02
ϵ	1.27 mm	31.36	0.55	-0.01
	2.54 mm	62.73	1.09	-.01
	-1.27 mm	-31.36	-.55	.01
	-2.54 mm	-62.73	-1.09	.01
δ	1.27 mm	-31.35	-0.27	0.00
	2.54 mm	-62.71	-.55	.00
	-1.27 mm	31.35	.27	.00
	-2.54 mm	62.71	.55	.00
γ, β	1°	-31.46	-0.55	-0.02
	2°	-64.04	-1.12	-.03
	-1°	30.42	.53	.01
	-2°	59.72	1.04	.02
Indexing head	1°	-30.96	-0.54	-0.01
	-1°	30.96	.54	.01

TABLE II

ERROR ANALYSIS VALUES

Misalinement parameter	k_1 ($\alpha = 2°$)	t	m	E_m
γ	123.84 μm	0.00834 deg	1 deg	1.03 μm
β	61.92 μm	.00834 deg	1 deg	.52 μm
θ	61.94 μm	.00834 deg	1 deg	.52 μm
ρ	61.74 μm	.00834 deg	1 deg	.52 μm
ϵ	62.72 μm	7.6 μm	1.27 mm	.37 μm
δ	62.70 μm	7.6 μm	1.27 mm	.37 μm
ϕ	Parabolic	.00834 deg		.02 μm
Root sum square	---------	----------	-------	1.47 μm
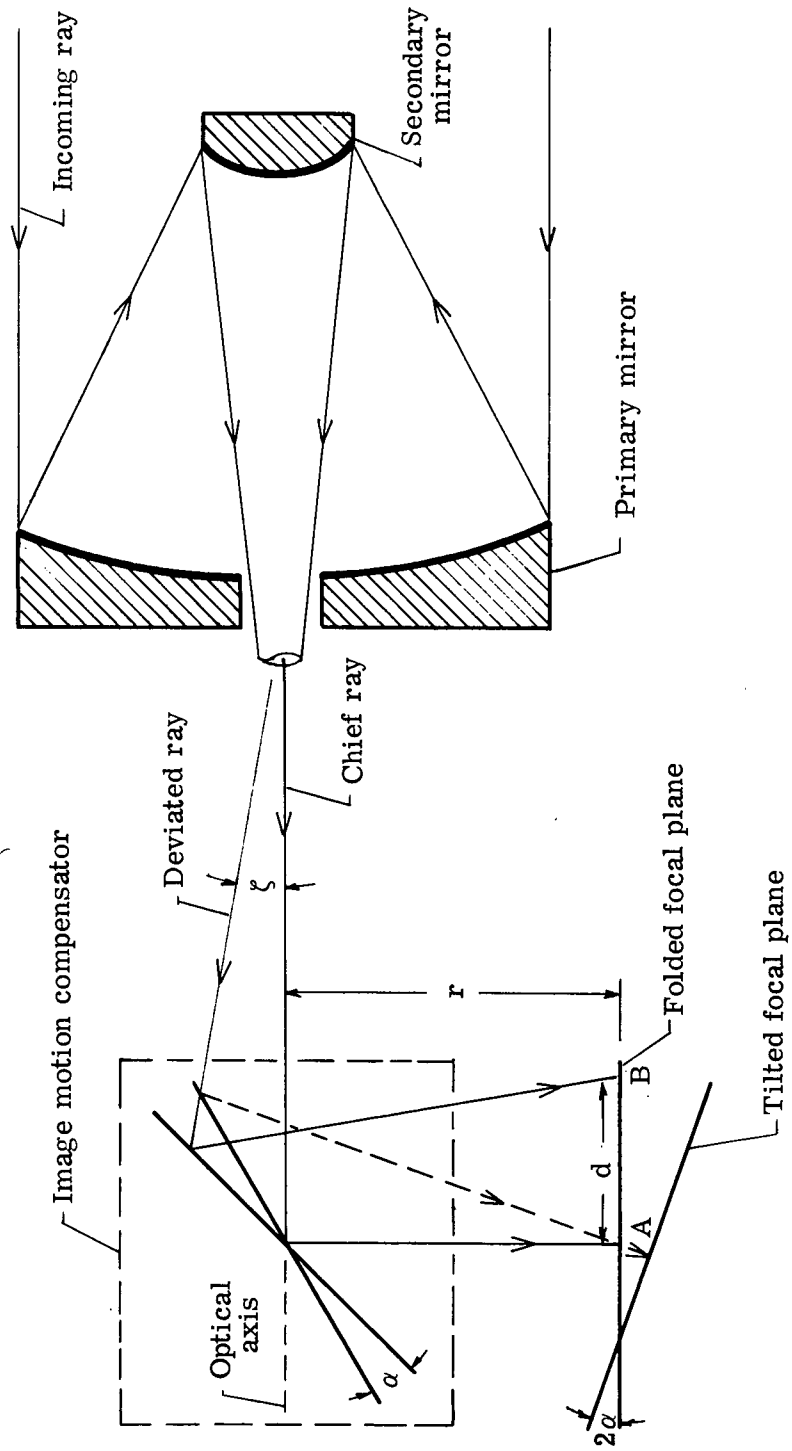
Figure 1.- Schematic representation of single-mirror image motion compensator.

17
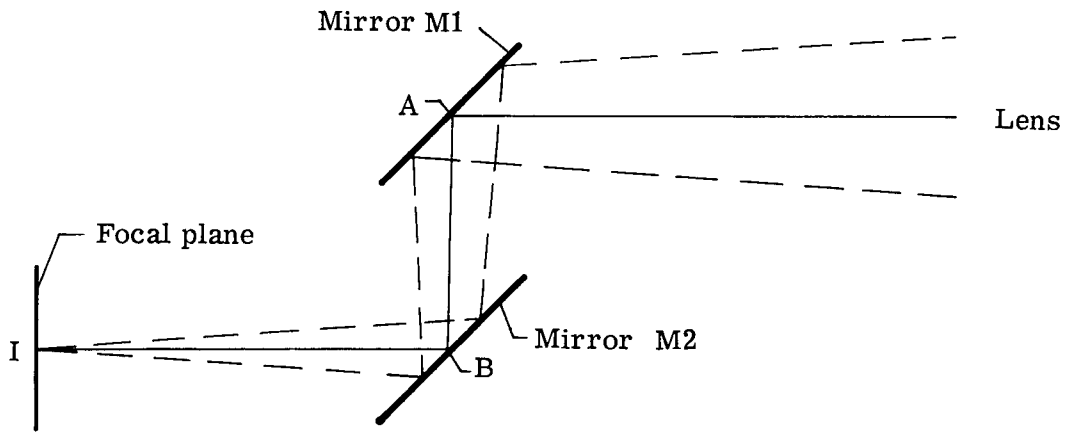
(a) Initial alinement.
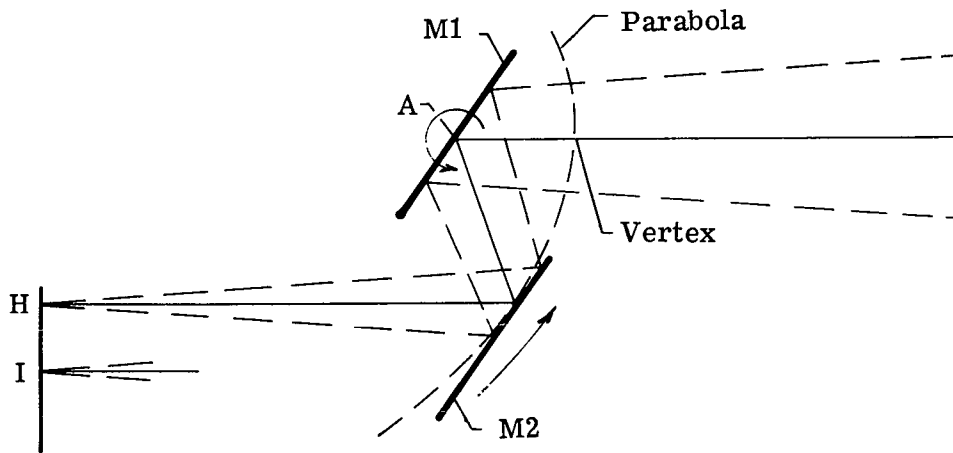
(b) Mirrors rotated.

Figure 2.- Schematic representation of image motion compensator.
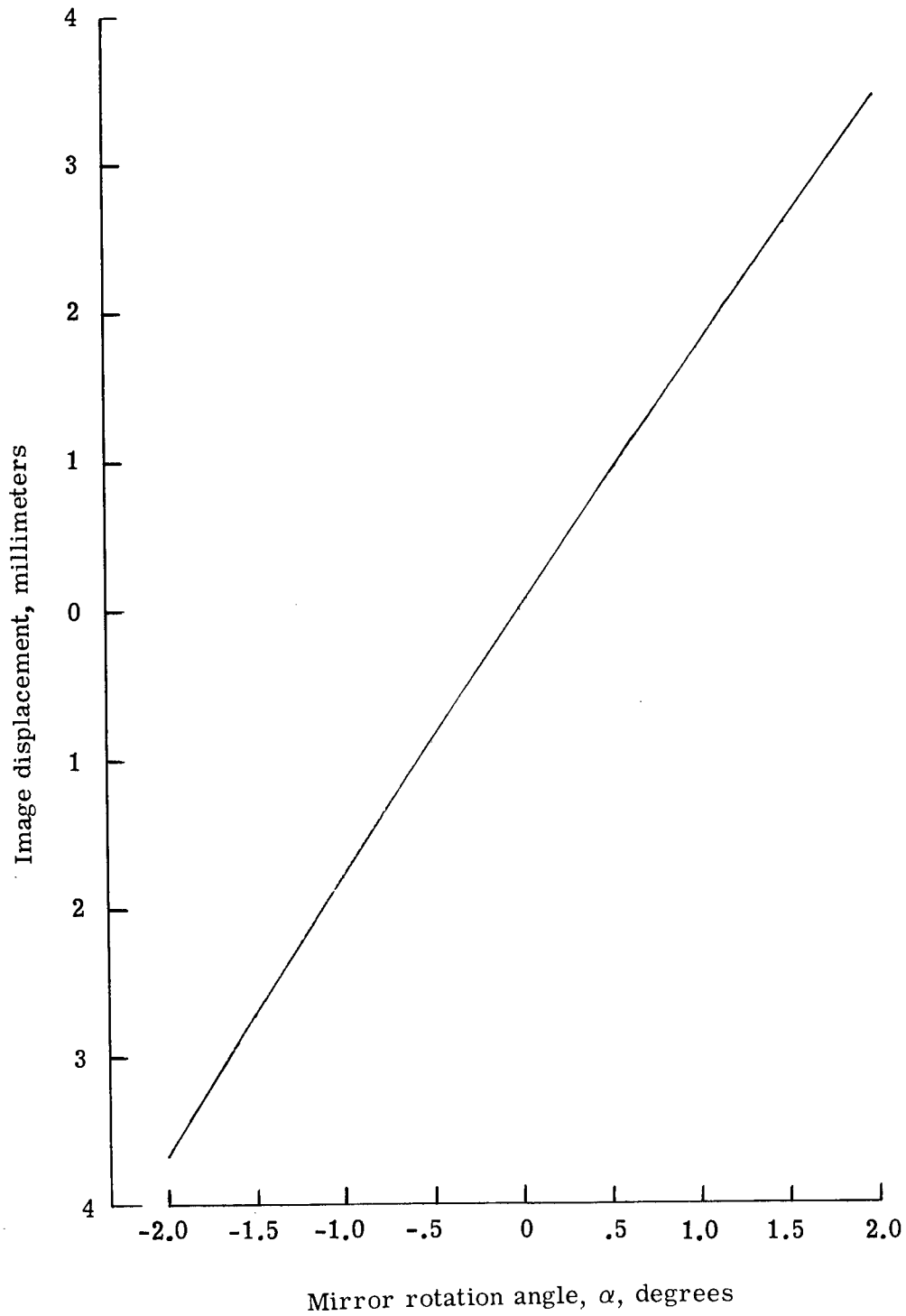
Figure 3.- Image displacement as function of mirror rotation angle.
p = 5.08 centimeters.
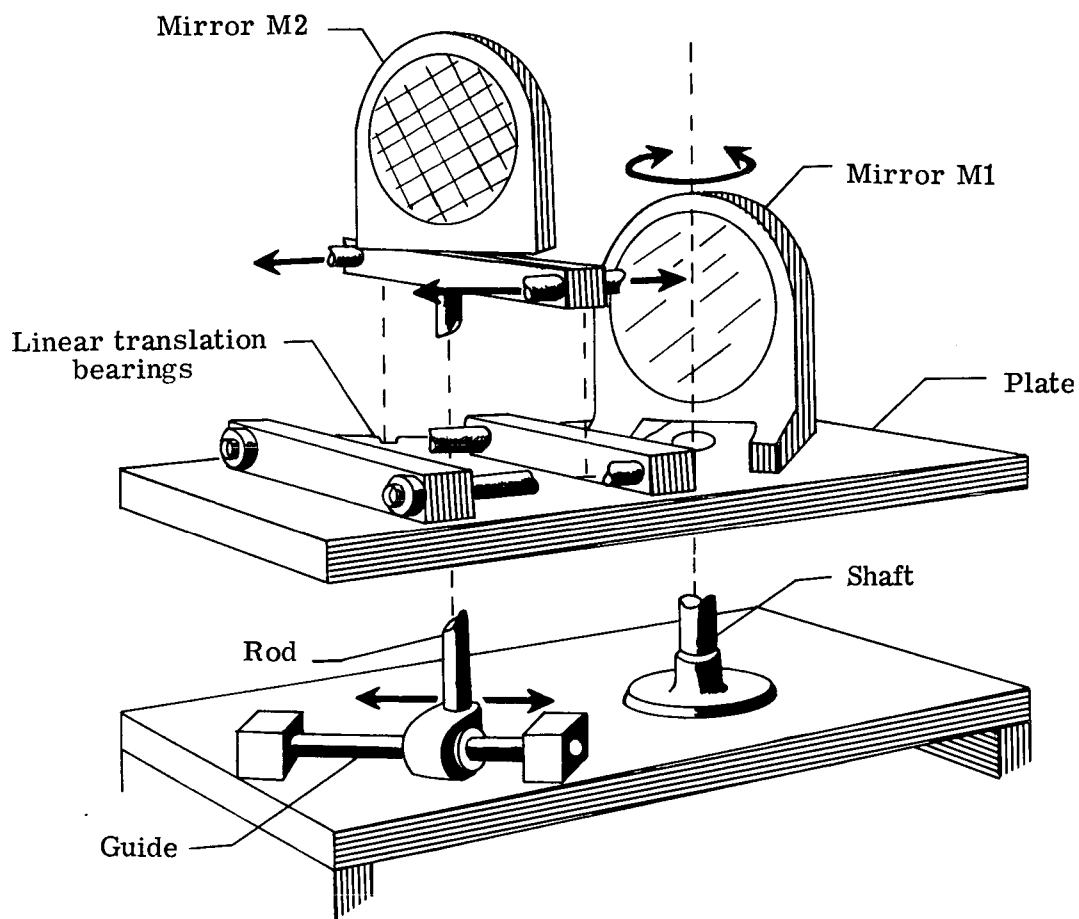
Figure 4.- Exploded view of the image motion compensator.

(a) γ.

(b) ϵ.

(c) β.

(d) θ.
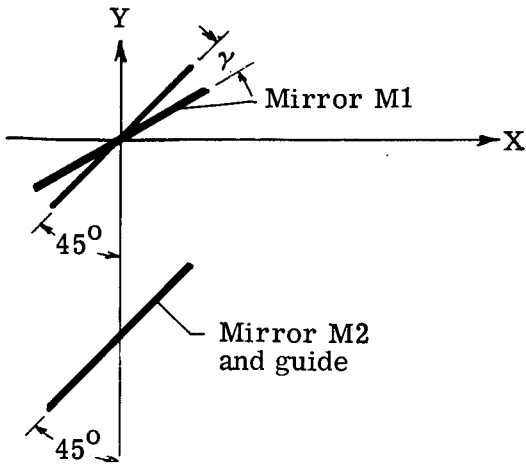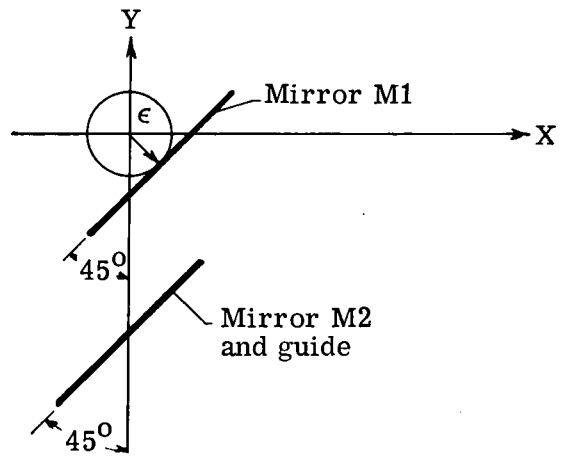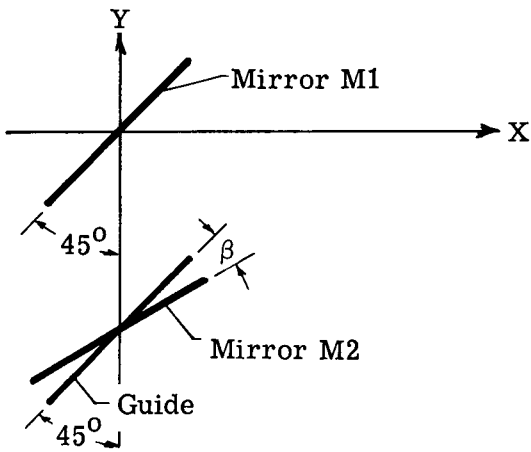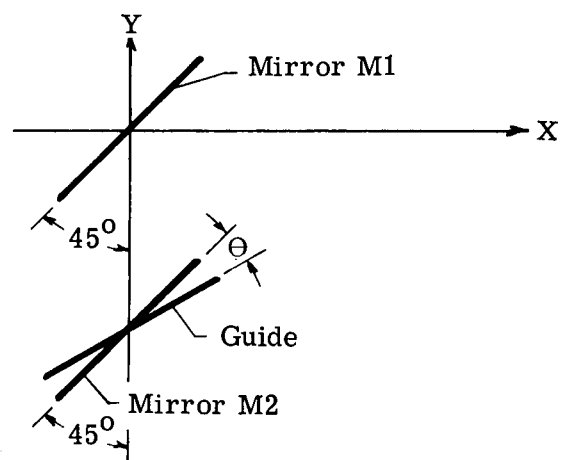
Figure 5.- Schematic representation of the misalinement errors of the image motion compensator.

(e) δ.

(f) ρ.

(g) φ.
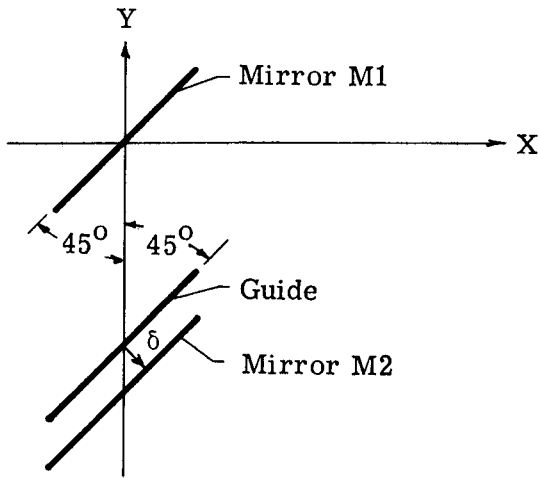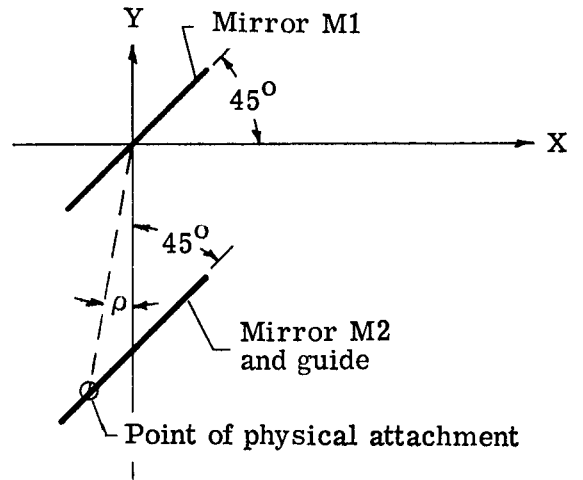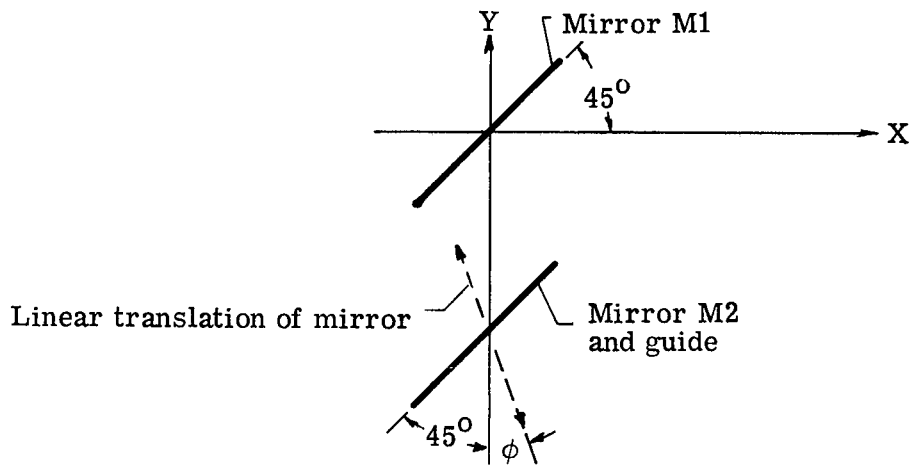
Figure 5.- Concluded.
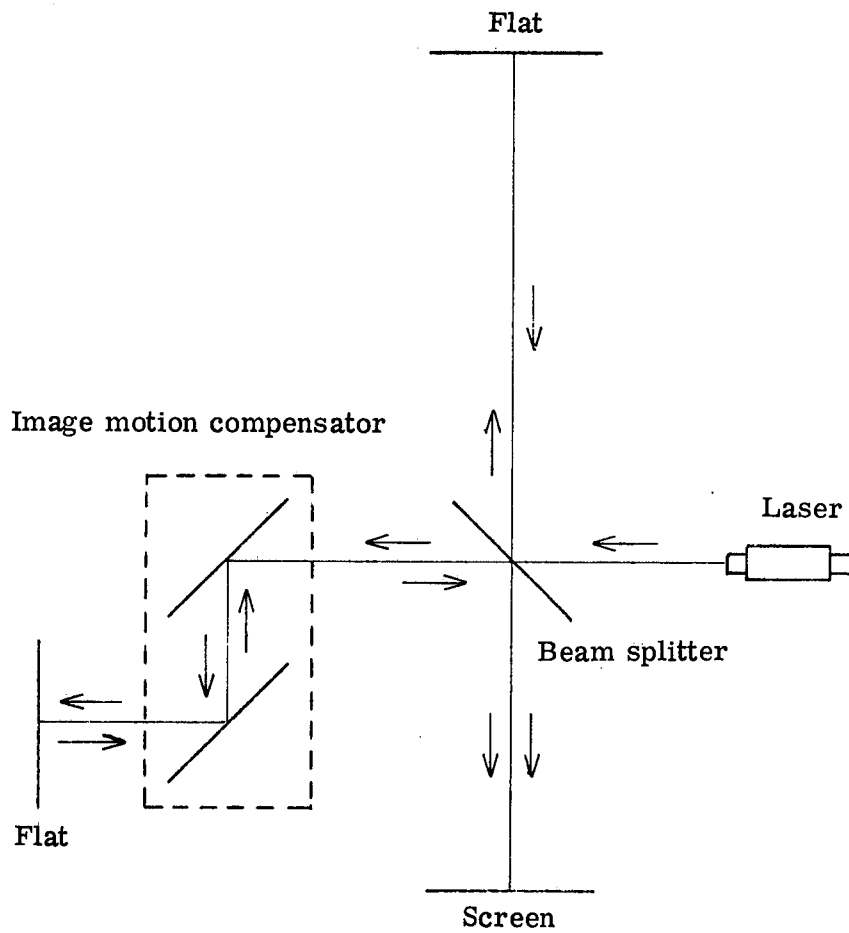
Figure 6.- Schematic diagram of interferometer system used
to evaluate system.
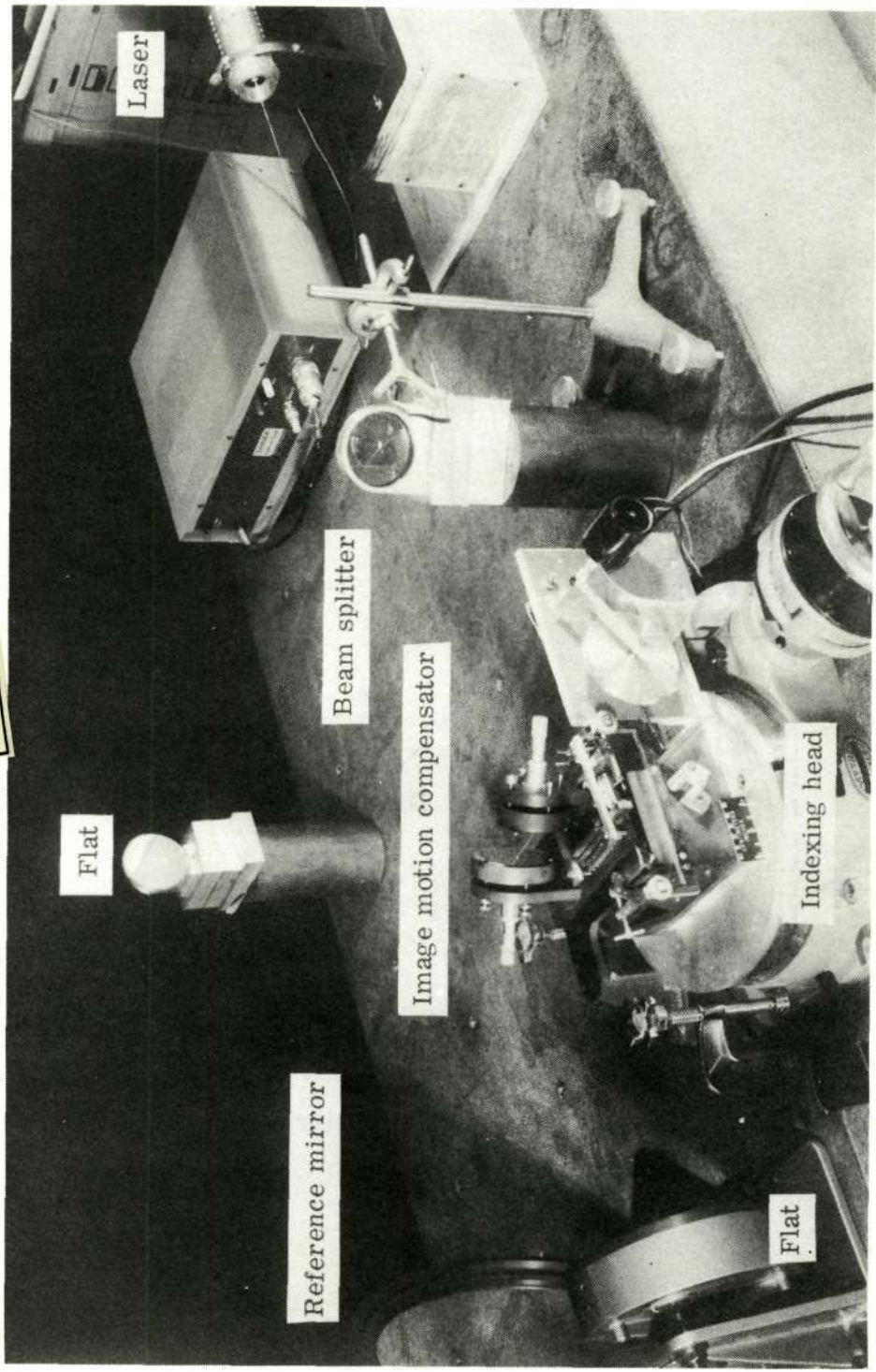
Figure 7.- Twyman-Green interferometer incorporating the image motion compensator.

L-68-3933.1

24
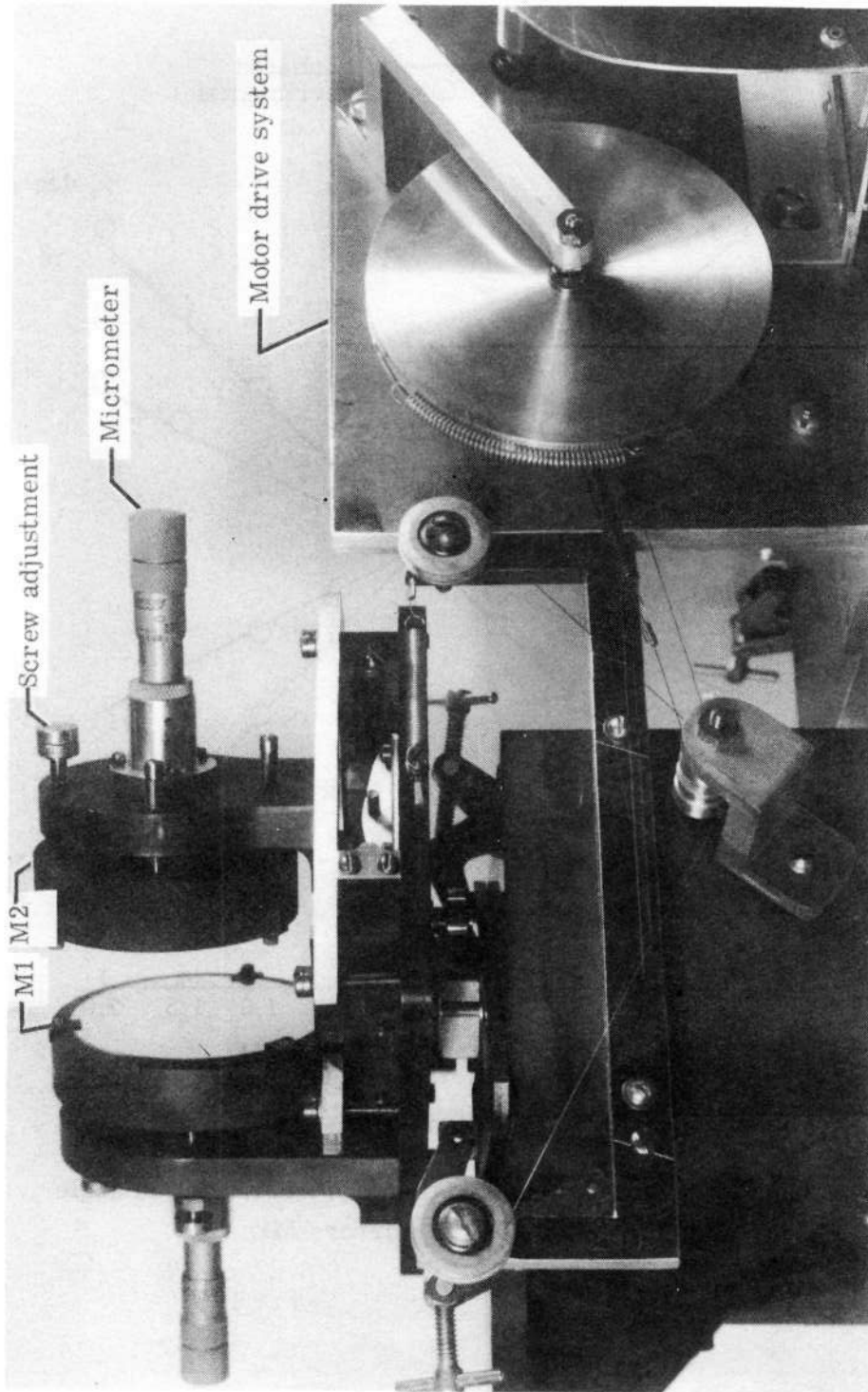
L-68-3934.1

Figure 8. - Experimental version of the image motion compensator.
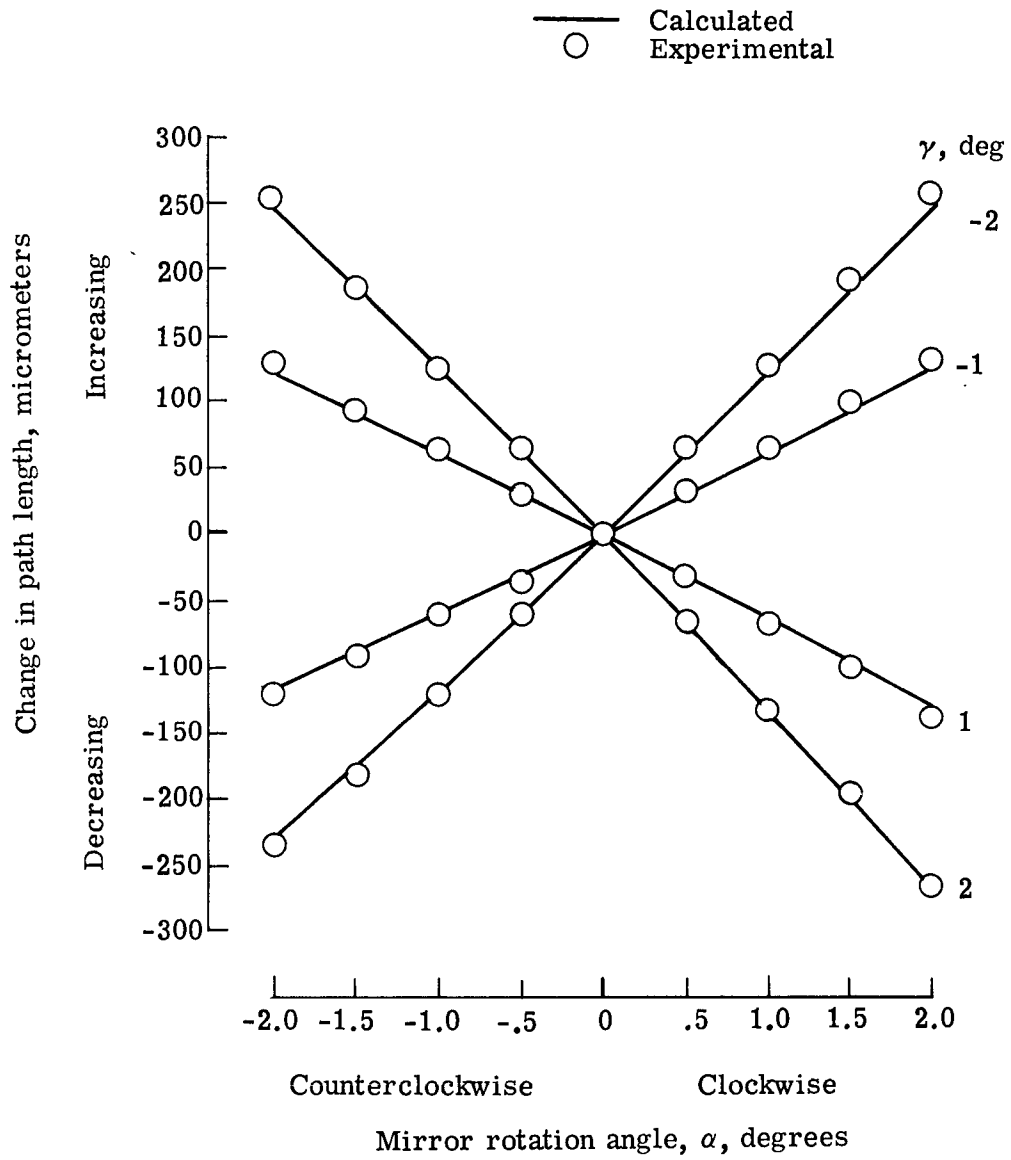
Figure 9.- Change in path length as function of mirror rotation angle
for misalinement angles in mirror M1.
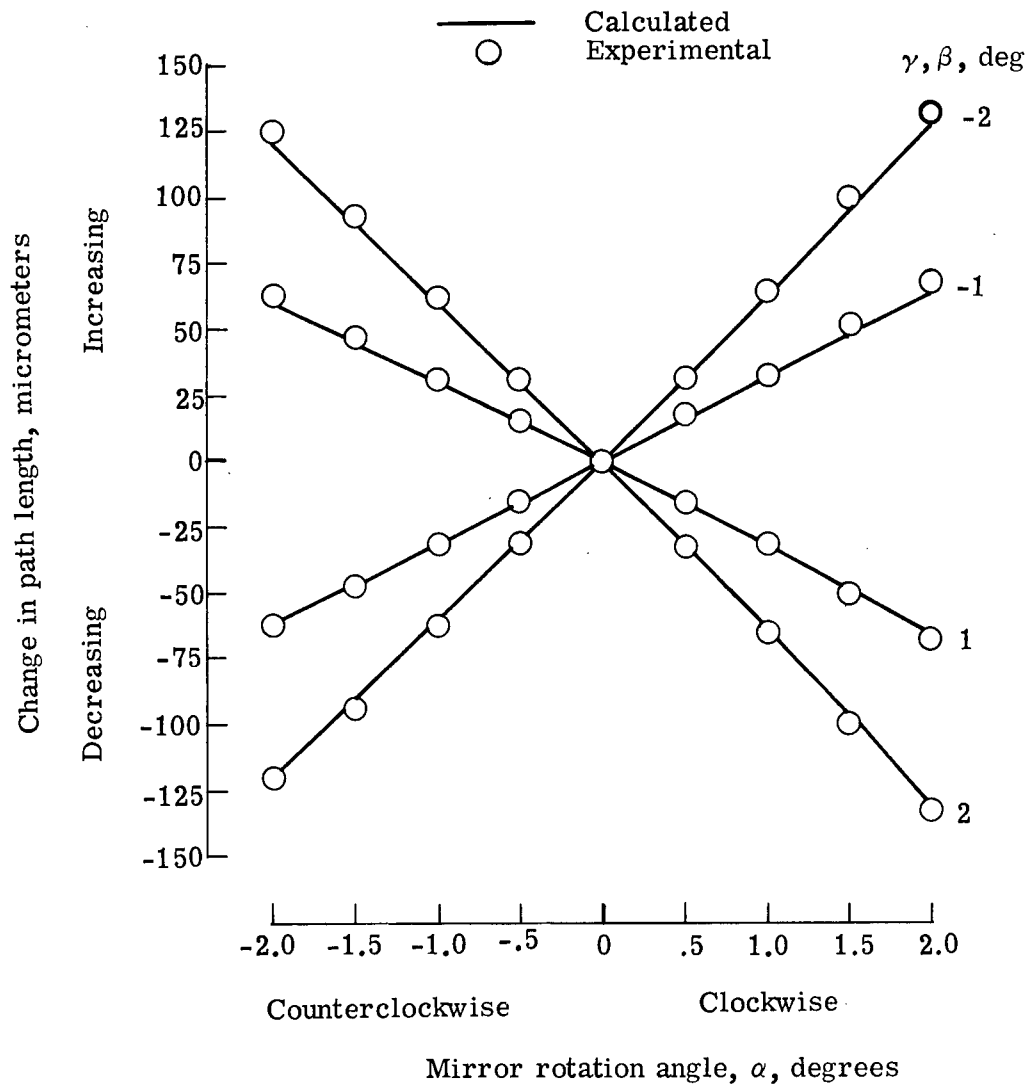
Figure 10.- Change in path length as function of mirror rotation angle for simultaneous misalinement errors in γ and β.
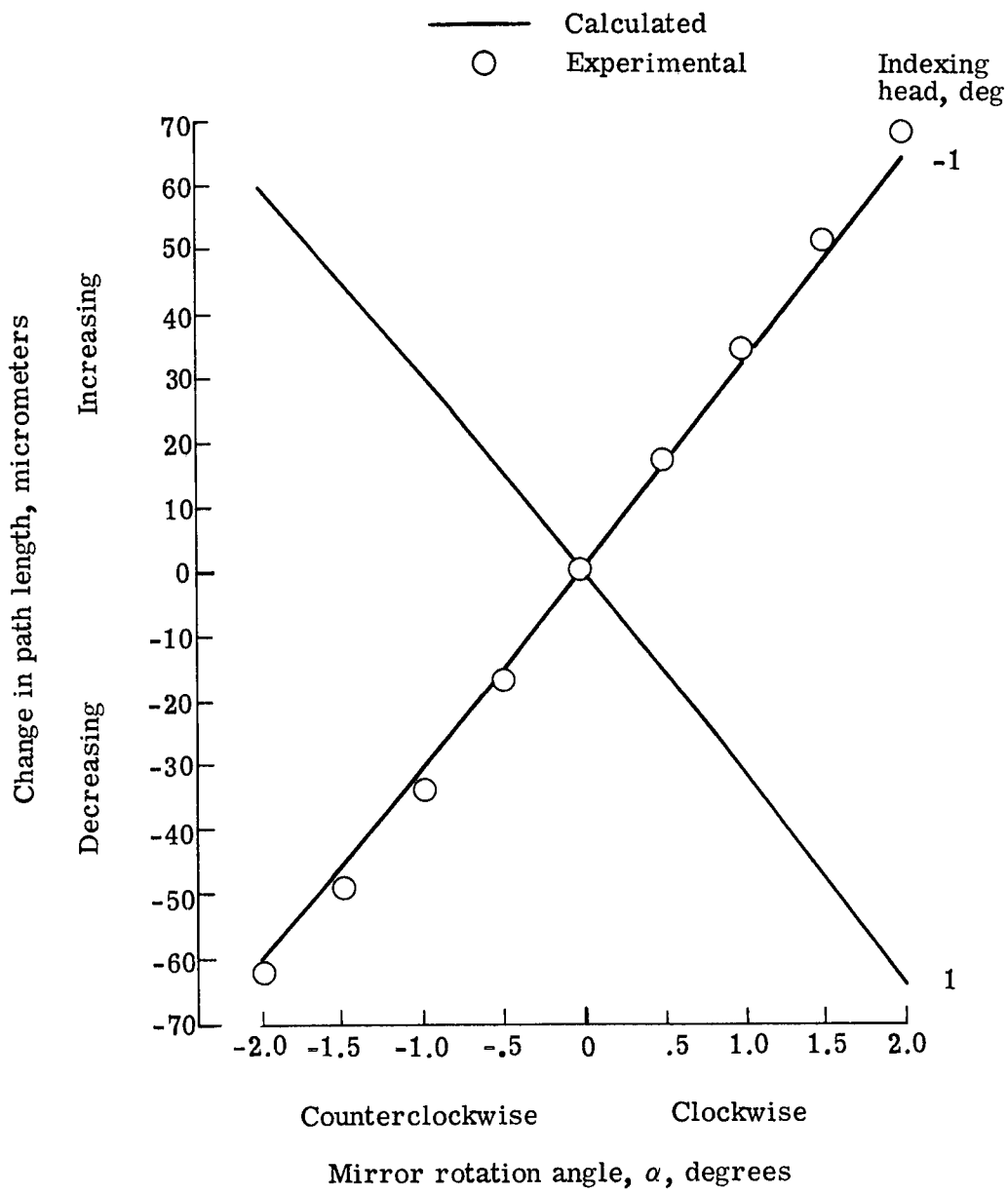
Figure 11.- Change in path length as function of mirror rotation angle for angular rotation of entire system.
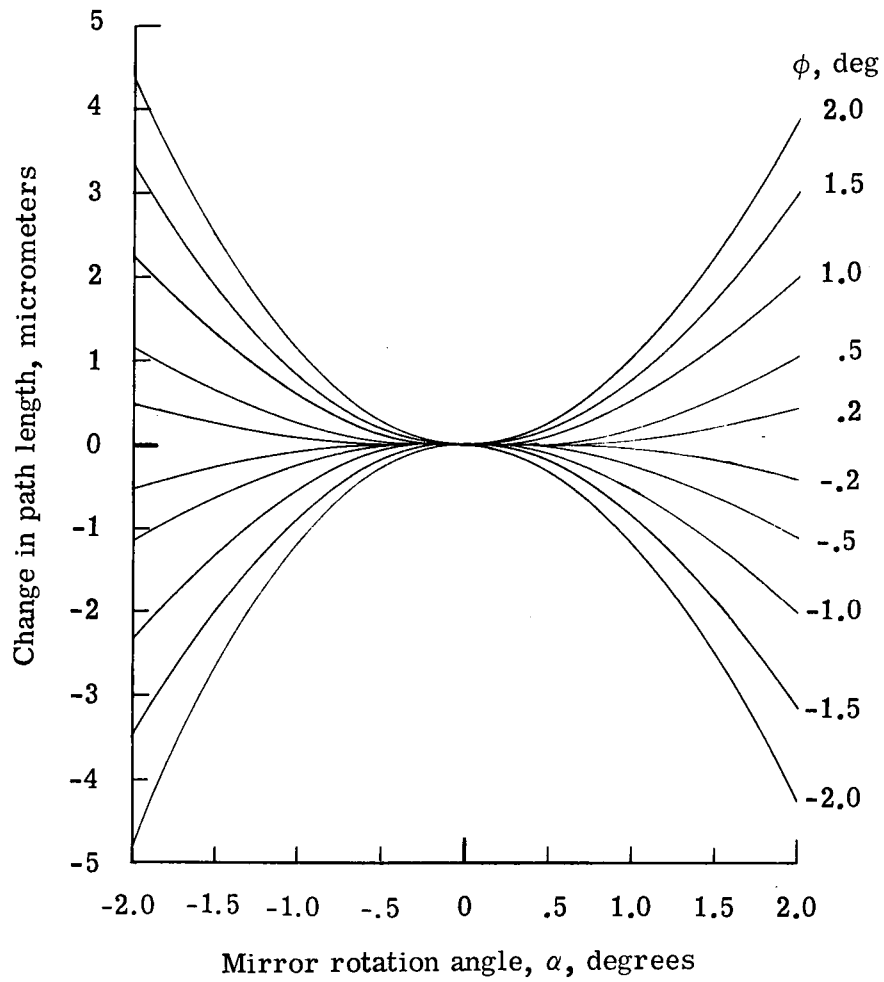
Figure 12.- Change in path length as function of mirror rotation
angle for nonlinear errors.
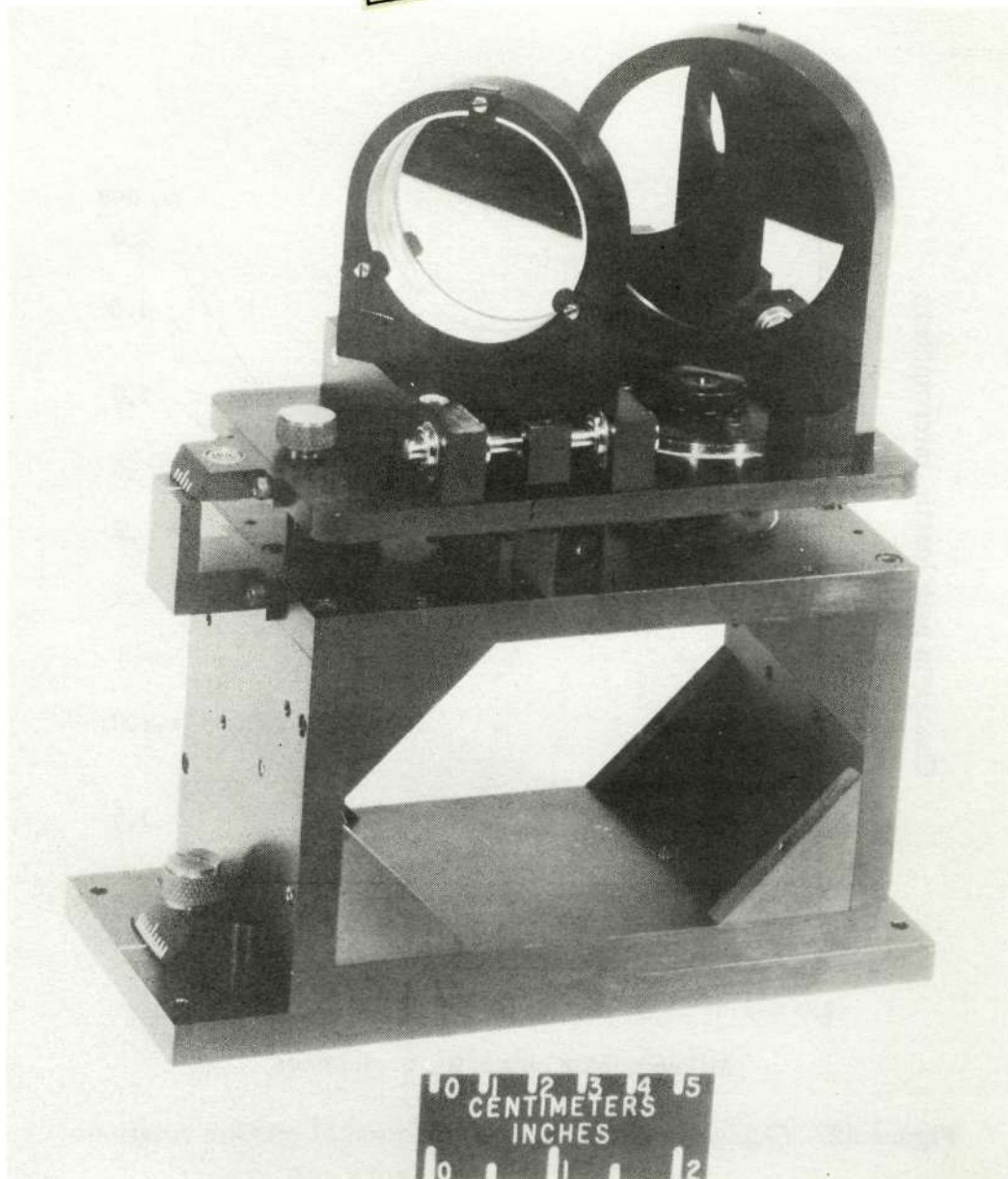
L-69-2322

Figure 13.- Image motion compensator.
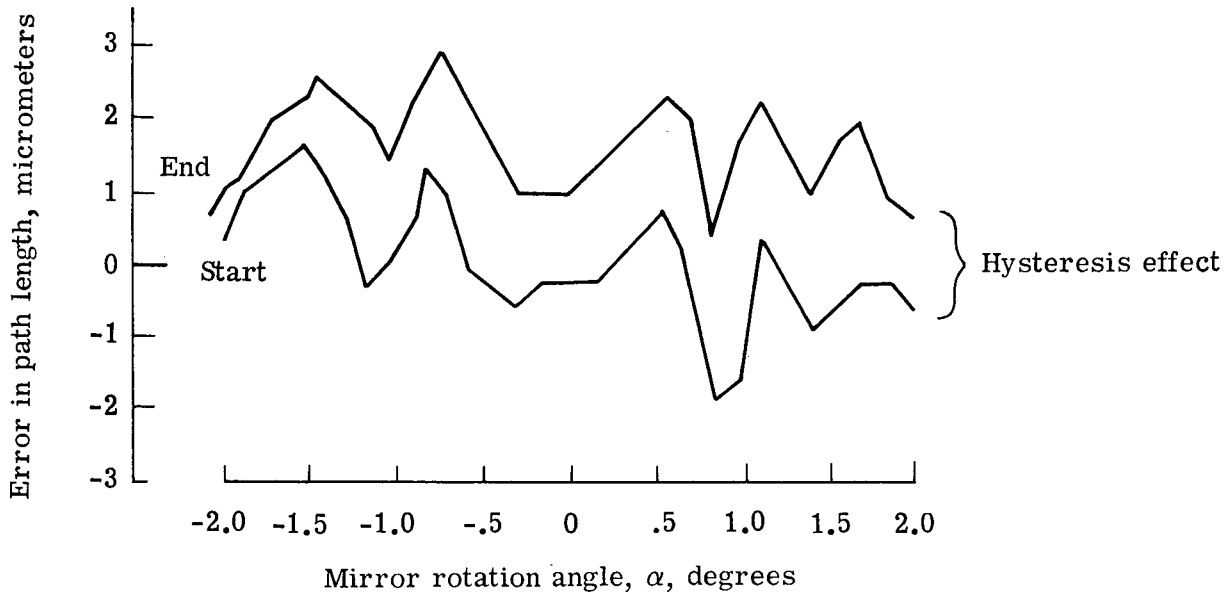
Figure 14.- Error in path length as function of mirror rotation angle
for best alinement.
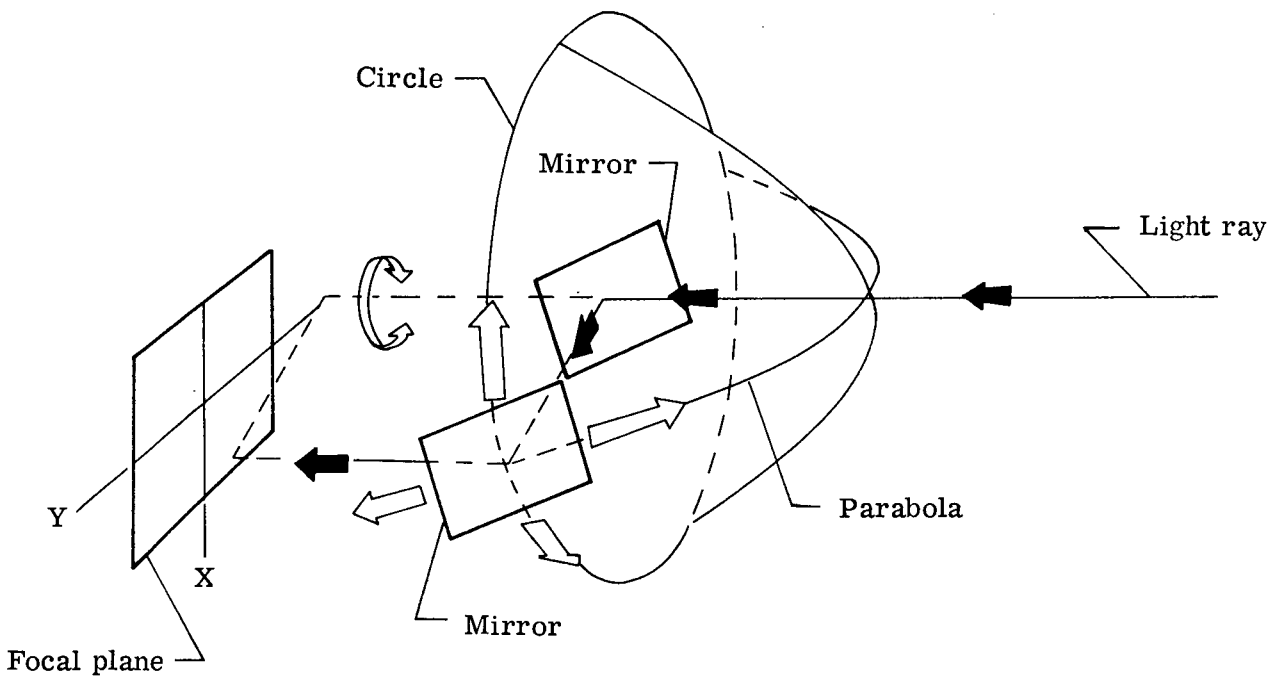
Figure 15.- Schematic diagram illustrating the two-axis technique.
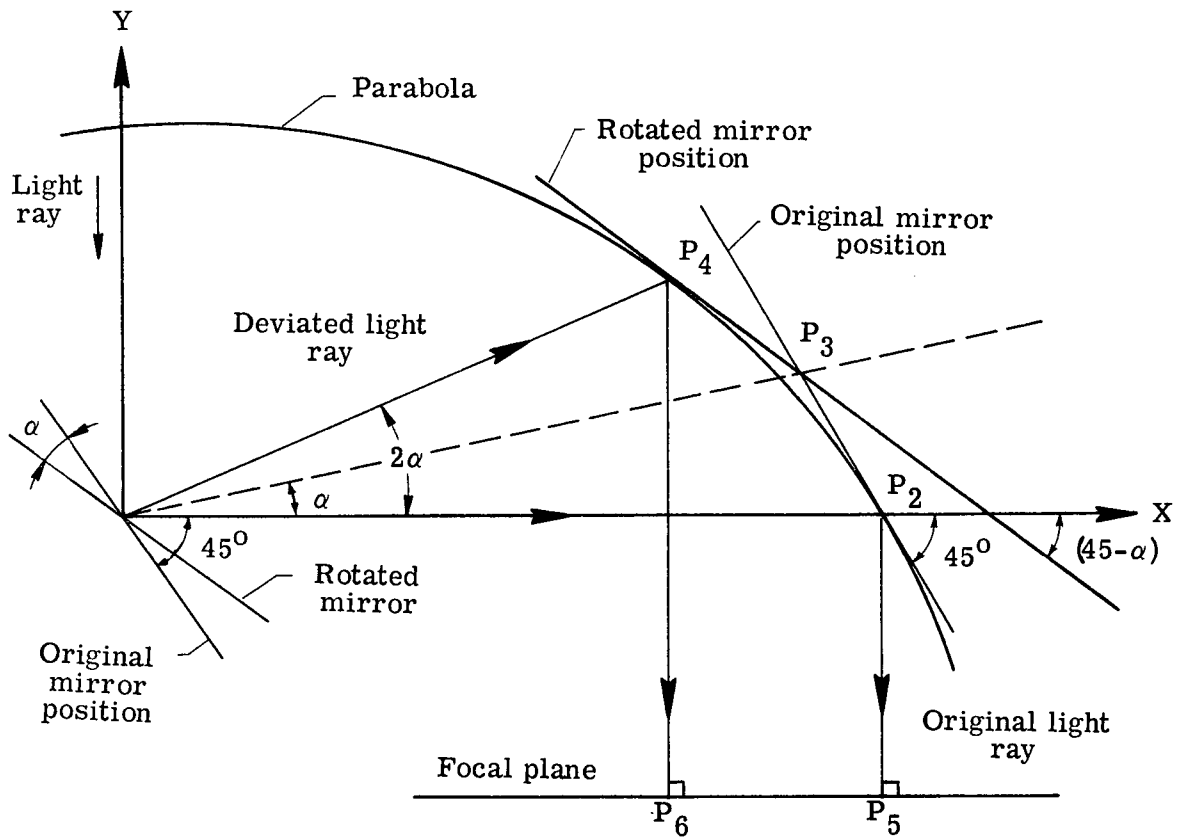
Figure 16.- Schematic representation showing image displacement as
function of mirror rotation.